Cultivar- and tissue-specific transcriptomic changes induced by cadmium in Brassica parachinensis

Yang Liu
Shenzhen University
Shuai Liu
Shenzhen University
Yanwu Deng
Shenzhen University
Chenjiang You
Shenzhen University
Weixin Zhang
Shenzhen University
Xuemei Chen
University of California Riverside
Lei Gao
Shenzhen University
Yulin Tang (yltang@szu.edu.cn)
Shenzhen University https://orcid.org/0000-0002-7098-8558

Research article

Keywords: Brassica, cadmium, chloroplast, microRNA, transcriptome, ion transporter

Posted Date: November 27th, 2019

DOI: https://doi.org/10.21203/rs.2.17772/v1

Abstract

Background One of the main pathways for cadmium (Cd) transfer from the environment to the human body is through the consumption of leafy vegetables, and Brassica leafy crops tend to be Cd hyper-accumulators. But its response strategies to Cd still lack of systematic study.

Results To investigate Brassica response strategies to Cd, we identified two cultivars with different Cd translocation efficiencies and performed mutli-transcriptomic sequencing studies under Cd treatments. Certain transporter families exhibited different temporal expression profiles in the two cultivars and may underlie the different Cd translocation efficiencies. Cd induced a drastic reduction of a 22 nt small RNA, the footprint of a pentatricopeptide repeat (PPR) protein on the chloroplast ndhB transcript and the concomitant down-regulation of the ndhB transcript. A global reduction in the expression of PPR genes was found, revealing previously unknown effects of Cd on organellar gene expression. Analyses of microRNAs (miRNAs) and their target genes by small RNA and degradome sequencing not only revealed Cd-induced changes in miRNAs but also implicated the existence of a regulatory cascade involving bra-miR156, its target gene, and bra-miR397 and bra-miR398 in Cd stress responses.

Conclusions The present findings help uncover the impact of Cd stress on the transcriptome of B. parachinensis and provide candidate genes and miRNAs for further investigation.

Introduction

Cadmium (Cd) is a widespread heavy metal that is easily released into the environment by human industrial activities (Sanità Di Toppi and Gabbrielli 1999). It can be transferred to and chronically accumulate in human bodies via the food chain, and one of the main pathways of Cd transfer from plants to humans is through leafy vegetable consumption (Huang et al. 2017). Brassica crop species include various leafy vegetables, including cabbages and pak choi. The hyper-tolerance and hyper-accumulation of Cd in Brassica species (Lin and Aarts 2012; Rizwan et al. 2018) increases the risk of human exposure to this heavy metal. Brassica parachinensis L.H.Bailey (Chinese flowering cabbage) is a Brassica leafy vegetable with a short vegetative cycle, large biomass and extensive planting adaptability (Qiu et al. 2011b). It has been recognized as a hyper-accumulator of Cd with different absorption ability depending on the genotype (Qiu et al. 2011a). Its Cd absorption and accumulation mechanisms warrant investigation.

Cd is a non-essential metal in plants. It is typically absorbed in roots and binds to organic acids and amino acids in the xylem vessels, followed by its transfer to the shoots via xylem (Nakamura et al. 2008; Wu et al. 2015; Khan et al. 2017). Its accumulation in plant cells can damage mitochondria, the photosynthetic apparatus, membranes and other cell parts (Lin and Aarts 2012). Studies over the last two decades have shown that plants avoid or endure Cd stress by chelating Cd (Wójcik and Tukiendorf 2011; Gielen et al. 2017), compartmentalizing and sequestering Cd (Zhang et al. 2018a), promoting Cd efflux (Verret et al. 2004; Zhang et al. 2016) and/or regulating Cd influx (Yao et al. 2018). Several families of

metal ion transporters, such as heavy metal ATPases (HMAs) (Zhang et al. 2016), natural resistance-associated macrophage proteins (NRAMPs) (Sasaki et al. 2012; Tang et al. 2017) and ATP-binding cassette subfamily C proteins (ABCCs) (Brunetti et al. 2015), have been implicated in the transport and sequestration of Cd. However, in some cases, the functions of individual members within the same family differ between non-hyper-accumulators and hyper-accumulators. For example, OsHMA3 sequesters Cd into vacuoles in rice roots to reduce its Cd levels in shoots, while SpHMA3 up-regulation in Sedum plumbizincicola enhances Cd tolerance and accumulation in shoots (Sasaki et al. 2014; Liu et al. 2017; Zhang et al. 2018a). In general, individual gene functions depend on the genetic background in a complex way, and transcriptome analyses have shown that Cd induces a wide range of changes in different biological pathways. These include transport (Feng et al. 2018), reactive oxygen species scavenging (Yu et al. 2017a; Xu et al. 2018), secondary metabolite biosynthesis (Chen et al. 2017), cell wall modification (Gao et al. 2013) and DNA or RNA damage (Xu et al. 2018). To understand how plant cope with Cd stress and the related mechanisms, it is essential to clarify the up- and downstream activities and factors related to genes in these biological pathways.

MiRNAs are small non-coding RNAs that post-transcriptionally regulate gene expression by transcript cleavage, translation inhibition or secondary siRNA biogenesis from the target gene transcripts (Yu et al. 2017b). They have been implicated in abiotic stress tolerance (Shriram et al. 2016), including the response to heavy metal stress in plants (Noman and Aqeel, 2017). Some Cd responsive miRNAs have been identified in rice (Wang et al. 2009; Ding et al. 2011), B. napus (Zhou et al. 2012a; Jian et al. 2018), B. parachinensis (Zhou et al. 2017), soybean (Fang et al. 2013) and the hyper-accumulator Sedum alfredii (Han et al. 2016). Additionally, specific functions of miR166 and miR395 in Cd accumulation and tolerance have been reported in rice and B. napus, respectively (Zhang et al. 2013; Ding et al. 2018). However, knowledge of miRNAs in Cd stress responses in B. parachinensis is rudimentary: only miRNA profiles under prolonged Cd treatments were examined and global detection of miRNA activities by degradome sequencing was not performed (Zhou et al. 2017).

To investigate the effect of Cd stress on B. parachinensis, two cultivars with different Cd translocation efficiency were treated with a relatively high concentration of Cd for a short period, and the mRNA and sRNA transcriptomes as well as degradomes in the roots and leaves were analyzed. Our results showed that roots of the two cultivars largely exhibited similar transcriptional responses to Cd, with many genes related to metal ion transport being up-regulated by Cd. On the other hand, changes in gene expression and sRNA abundance were affected differently in the leaves of the two cultivars. The differences in Cd response in leaves were consistent with differences in their root-to-shoot Cd translocation capacity. The sRNA sequencing revealed a drastic reduction of an RNA footprint of a chloroplast pentatricopeptide repeat (PPR) protein and the concomitant reduction in the levels of the transcript from which the footprint originated. This, and the induction of many PPR genes by Cd, suggested that Cd induces changes in chloroplast RNA metabolism through nucleus-encoded and chloroplast-localized PPR proteins. Our sRNA-seq not only uncovered many novel miRNAs, but also identified many conserved and none-conserved miRNAs being regulated by Cd stress. In addition, degradome sequencing revealed the effects of these miRNAs in Cd response. Three miRNA-target modules seem to have regulatory relationships and form a

gene expression cascade in Cd stress response. These genes and miRNAs can help to provide new potential directions for the breeding of food-safe Brassica crops.

Material And Methods

Plant materials and Cd treatment

Six *B. parachinensis* cultivars were used in this experiment. Cultivars YQ, YLCT and JY40 were bought from the Vegetable Research Institute of Guangdong Academy of Agricultural Sciences. YQ80, TC and PT45 were obtained from Guangzhou Academy of Agricultural Sciences, Lianzhou Fengyu Agricultural Technology Co., Ltd., and Guangzhou Yangxin Seedling Co., Ltd., respectively. Seeds were sown in vermiculite and watered with 1/4 Hoagland nutrient solution. After 7 days (d), the seedlings were transferred to a simple hydroponic culture device with 1/2 Hoagland nutrient solution. After 8 d in hydroponic culture, Cd (Cd^{2+}) stress was applied by adding $Cd(NO_3)_2$ to the nutrient solution with final Cd^{2+} concentrations of 50 *μM* or 5 *μM*. The nutrient solution was changed every 3 d.

Biomass and Cd content determination

Fifteen-day-old seedlings were used for Cd treatment. Roots and shoots were collected separately at the designated time points to determine the biomass and Cd content. Tissue samples (0.5-1.0 g) were oven-dried then digested with 10 mL 65% HNO_3 using the Microwave Digestion System (EthosONE, Milestone, Italy). Cd contents were analyzed by inductively coupled plasma optical emission spectrometry (ICP-OES, Optima 7000DV, Perkin Elmer, USA). Three biological replicates were detected.

mRNA sequencing and data analysis

Fifteen-day-old TC and YQ seedlings were treated with 50 *μM* Cd. Roots and the first pair of leaves were separately harvested at 0, 24 and 48 HAC then immediately frozen in liquid nitrogen for total RNA extraction. Three biological replicates were performed for each time point, with each biological replicate consisting of three seedlings grown in different hydroponic growth containers.

Total RNA was extracted using TRI Reagent (Molecular Research Center, Inc.). RNA-seq libraries were prepared and sequenced by Beijing Novogene Co., Ltd. using the Illumina HiSeq 2500 platform to obtain 150 bp paired-end reads. Data analysis was performed using the pRNASeqTools pipeline (https://github.com/grubbybio/pRNASeqTools) in its mrna mode. First, the raw reads were trimmed using cutadapt (Martin 2011) with default settings, then the trimmed reads were mapped to the *Brassica rapa* v2.0 genome (Cai et al. 2017) using STAR (Dobin et al. 2013). Second, the read counts of both introns and exons were combined as the total read count of one transcript using pRNASeqTools. Transcript levels were measured and normalized in TPM (transcripts per million) using TBtools (Chen et al. 2018) (https://github.com/CJ-Chen/TBtools/releases). Finally, DEGs were identified using DEseq2 with a fold change of 1.5 and *P*-value < 0.01 as the cutoff parameters (Love et al. 2014). Coding sequences (CDSs) of genes from the *B. rapa* v2.0 genome was compared against the Swiss-Prot protein sequence database

(Bairoch and Apweiler 2000) using blastx with e-value < 1e-5 as the cutoff parameters (Camacho et al. 2009) to derive the functional descriptions of genes. Gene ontology (GO) annotations were performed using GOanna tools available at the AgBase v2.0 website (http://agbase.arizona.edu/index.html) (McCarthy et al. 2011). GO enrichment analysis of DEGs was performed using TBtools (Chen et al. 2018) with Fisher's exact test. REVIGO was used to remove the duplicated GO terms (Supek et al. 2011). Trend analyses of gene expression at 0, 24 and 48 HAC were accomplished using the Short Time-series Expression Miner software (STEM) (Ernst and Bar-Joseph 2006) at the OmicShare tools website (http://www.omicshare.com/tools). The cluster dendrogram and correlation coefficient matrix of all samples were respectively plotted using the 'hclust' and 'heatmap' R functions, and volcano plots of the DEGs were generated using 'ggplot2' in R (Wickham 2016). The above clustering analyses revealed that one biological replicate of each of the samples, YQ roots at 24 HAC, YQ roots at 48 HAC, YQ leaves at 0 HAC, TC leaves at 24 HAC and TC leaves at 48 HAC, was an outlier, only two biological replicates of these samples were retained for DEG analyses.

sRNA-seq library construction and data analysis

To construct sRNA-seq libraries, 20 μg of total RNA was resolved on a 15% urea-PAGE gel, and the ~10-40 nt region was excised from the gel. sRNAs were recovered by shaking the smashed gel in 0.4 M NaCl-DEPC overnight, followed by precipitation in a mixture containing glycogen, sodium acetate and ethanol. sRNA libraries were constructed following the instructions for the NEB Next Multiplex Small RNA Library PrepSet for Illumina kit (NEB E7300). The libraries were sequenced on an Illumina HiSeq 2500 instrument using a 50 bp single-read strategy by Beijing Berry Genomics Co., Ltd. sRNA data analysis was performed using the pRNASeqTools pipeline in its srna mode (Jia et al. 2017). The sequencing data were processed to remove the adapter sequence (AGATCGGAAGAGC) using cutadapt (Martin 2011). The trimmed reads were mapped to the reference genome, which included the *B. rapa* v2.0 chromosomes, mitochondrial genome sequence (GenBank accession: JF920285) and chloroplast genome sequence (GenBank accession: DQ231548, Wu *et al.* 2012), using ShortStack with default parameters (Axtell 2013). Normalization was performed by calculating the RPMR (reads per million of 45S rRNA reads) value (Li et al. 2016). The reference genome was tiled into 100 bp windows as individual bins, and reads whose 5' end nucleotides fell within a given bin were assigned to this bin (Li et al. 2016). Annotations for genes and TEs were downloaded from the *Brassica* Database (http://brassicadb.org/brad/index.php), and rRNAs were located by aligning known full-length rRNAs of plants onto the *B. rapa* v2.0 genome. As the *B. rapa* v2.0 genome does not contain *MIR* gene annotations, we annotated *MIR* genes by the alignment of *MIR*/miRNA annotations from the *B. rapa* v1.5 genome with the v2.0 genome (Sun et al. 2015). Prediction of novel miRNAs was performed using the *MIRNA* analysis mode of ShortStack (Axtell 2013), and only the novel *MIR* loci identified in at least two libraries were retained. DEMs were identified using DEseq2 with a fold change of 1.5 and *P*-value < 0.01 as the cutoff parameters (Love et al. 2014).

Degradome/PARE library construction and data analysis

Total RNA was used for degradome/PARE library construction. Equal amounts of total RNA from the samples at 24 HAC and 48 HAC were mixed as the Cd-treated samples. A total of 24 degradome/PARE libraries including three biological replicates were constructed using 75 μg of total RNA (Zhai et al. 2014). The libraries were sequenced using a 50 bp single-end read strategy on an Illumina HiSeq 2500 instrument at Beijing Berry Genomics Co., Ltd. The adapter sequences (TGGAATTCTCGGG) were removed, and reads shorter than 19 nt were filtered out using cutadapt (Martin 2011). Trimmed fastq files were converted to fasta files, and the degradome sites and the corresponding trigger miRNAs were identified using CleaveLand4 (Addo-Quaye et al. 2009). Degradome sites were selected with degradome category = 0 and degradome *P*-value < 0.05 as the cutoff parameters. MiRNA cleavage sites identified in at least two biological replicates were retained and were then manually screened using their T-plots. The miRNA cleavage sites with high background noise in the T-plots were removed.

sRNA gel blotting and quantitative RT-PCR

Hydroponic TC and YQ seedlings were prepared as described above, and the samples were harvested at 0, 24 and 48 HAC with three biological replicates. Total RNA was extracted using TRI Reagent, and 20 μg total RNA was resolved in a 15% urea-PAGE gel. sRNA gel blotting assay was performed using a method with enhanced sensitivity (Pall and Hamilton 2008). Biotin-labeled antisense DNA oligonucleotides were used to detect sRNAs. The DNA oligonucleotide probes are listed in Table S1.

Total RNA was reverse-transcribed into single-stranded cDNA using the PrimeScript™ RT reagent kit with gDNA Eraser (Perfect Real Time) (TAKARA Bio Inc.) with oligo (d)T primer and random 6-mers according to the manufacturer's instructions. Quantitative RT-PCR (qRT-PCR) was performed with biological duplicates and technical triplicates using TB™ Green Premix Ex Taq™ (TAKARA Bio Inc.) on the StepOnePlus Real-Time PCR System. *Actin 7* (*ACT7*, KU851921) from *Brassica rapa* subsp. *chinensis* was used as an internal reference gene (Wang et al. 2016), and the primers used for qRT-PCR are listed in Table S1.

Data availability

The sequencing data have been deposited into the NCBI Sequence Read Archive (SRA, http://www.ncbi.nlm.nih.gov/sra) under the BioProject ID PRJNA513391.

Results

Different responses to Cd in two *B. parachinensis* cultivars

Fifteen-day-old seedlings of six widely grown *B. parachinensis* cultivars (YQ, YLCT, YQ80, TC, JY40 and PT45) were treated with 50 *μM* Cd for 6 d then analyzed for Cd accumulation and biomass. No significant difference was observed in the Cd content in roots and shoots among the six cultivars (Fig. S1a). The shoot biomass of all six cultivars was significantly reduced compared to the respective 0 *μM*

Cd controls (Fig. S1b). In contrast, changes in root biomass varied in the different cultivars: it was significantly reduced in TC and YQ80 and increased in YQ compared to the controls (Fig. S1b). An increase in root biomass in YQ but a decrease in TC after Cd stress was obvious upon visual inspection (Fig. S1b and c). Based on the different responses to Cd, the YQ and TC cultivars were selected for further analysis.

The Cd content in YQ and TC seedlings during the initial 48 hours after Cd stress (HAC) was measured to determine if there were any differences in Cd absorption and translocation between the two cultivars. In both cultivars, the shoot Cd content continuously increased from 6 to 48 HAC, while the root Cd content was steady from 6 to 24 HAC then rapidly increased at 48 HAC (Fig. 1a). One difference between the cultivars was the significantly higher shoot Cd content in YQ than TC at 12 HAC (Fig. 1a). The Cd content results implied that root-to-shoot Cd translocation mainly occurred within 24 HAC in both cultivars and that this translocation was more rapid in YQ than in TC at 12 HAC (Fig. 1a). To validate the observed differences, we performed another treatment with a lower Cd concentration (5 *μM*) for a longer time (3 d and 6 d). At both 3 d and 6 d, there were significant differences in the shoot Cd content between YQ and TC (Fig. 1b), indicating more efficient Cd translocation in YQ than TC. Taken together, the findings show that *B. parachinensis* YQ and TC respond differently to Cd stress in terms of root growth and Cd translocation efficiency.

Cd-induced mRNA transcriptome changes in TC and YQ leaves and roots

To further investigate the response strategies of *B. parachinensis* to Cd stress, leaves and roots of 15-d-old YQ and TC seedlings treated with 50 *μM* Cd were harvested at 0, 24 and 48 HAC for mRNA sequencing (mRNA-seq) analysis. As *B. parachinensis* is considered a variety of *Brassica rapa* (Cheng et al. 2016a), the sequencing reads from the mRNA libraries were mapped to the *B. rapa* genome (version 2.0) (Cai et al. 2017), resulting in 89.17% to 93.98% total mapped reads (Table S2). Analysis of differentially expressed genes (DEGs) showed that the DEG numbers and the trend of up- and down-regulation were similar in TC and YQ roots but differed noticeably in the leaves of these two cultivars (Fig. S2a and b). For example, there were more DEGs in YQ leaves than in TC leaves (Fig. S2b). In contrast to the considerable overlap of root DEGs between the two cultivars and at different Cd treatment time points, in leaves, YQ-specific DEGs were more than the overlapping DEGs between YQ and TC or the TC-specific DEGs (Fig. S2c). Cluster dendrogram and correlation coefficient analyses of the mRNA-seq data showed that YQ leaves at 24 HAC and 48 HAC constituted one cluster, and TC leaves at 0 HAC, 24 HAC and 48 HAC constituted another cluster (Fig. S3a and b). On the other hand, YQ and TC roots at 0 HAC were in one cluster, and YQ and TC roots at 24 HAC and 48 HAC were in another cluster (Fig. S3c and d). These data indicate that Cd stress had a more evident impact on gene expression in YQ leaves than TC leaves while roots of the two cultivars responded to Cd similarly.

The DEGs were further grouped according to the patterns of their expression changes over time (i.e., temporal expression profiles). The results showed that the significant profiles ($p < 0.05$) were similar between TC and YQ roots but different between TC and YQ leaves (Fig. 2a). For TC leaves, the most

significant profile was Profile 3, in which expression decreased then increased, followed by Profile 4, in which expression increased then decreased. The enriched GO terms for genes in Profile 3 were mostly related to basal metabolism, such as “cellular amide metabolic process”, “cellular nitrogen compound metabolic process” and “gene expression” (Fig. 2b and Table S3), suggesting that basal metabolism in TC leaves was initially negatively influenced then recovered. The enriched GO terms for Profile 4 genes were related to signaling and stimulus response, such as “gene expression”, “signaling” and “regulation of cellular process” (Fig. 2b and Table S3), suggesting that these biological processes were initially enhanced in TC leaves then returned to normal levels. In YQ leaves, basal metabolism related genes were clustered in Profile 2, in which expression decreased then stabilized, and genes related to signaling and stimulus response were mostly found in Profile 5, in which expression increased then stabilized (Fig. 2b and Table S3). The different expression trends of these similar groups of genes in TC and YQ leaves indicate that the impact of Cd stress on leaves persisted in YQ for a longer time but recovered more rapidly in TC.

In roots, the related genes in GO terms “metal ion transport”, “transmembrane transport”, “drug transmembrane transport”, “divalent metal ion transport” and “transition metal ion transport” were significantly enriched among Profile 5 (increased then stabilized expression) and Profile 6 (increased expression) in both TC and YQ (Fig. S4 and Table S4). The finding that Cd affected genes related to transmembrane transport suggests that these genes are involved in Cd response.

DEGs in response to Cd were related to metal ion transport and transmembrane transport

Cd absorption and translocation require transporter genes. We found that many of the DEGs with the GO term “metal ion transport” were members of the zinc/iron transporter (ZIP) family, the copper transporter (COPT) family and the HMA family (Table S5). For DEGs with the GO term “transmembrane transport”, some of them were found to belong to the ATP-binding cassette transporter B subfamily (ABCB family), ATP-binding cassette transporter C subfamily (ABCC family) and the yellow stripe-like (YSL) family (Table S5). We focused on these DEGs to examine their temporal expression profiles in response to Cd in shoots and roots. Most genes in the ABCC, ABCB, vacuolar cation/proton exchanger (CAX), COPT, HMA, ZIP and YSL families and all of the genes in the ABCG family were more highly expressed in roots than in leaves (Fig. 3). Although most of these genes had similar expression profiles in YQ and TC, several of them had different expression profiles in the two cultivars. For instance, six genes in the ABCC family (*ABCC3-3*, *ABCC3-1*, *ABCC1-2*, *ABCC15*, *ABCC4-1* and *ABCC7*) were up-regulated in YQ leaves at 24 HAC but not in TC leaves, and *HMA2-1* and *HMA3* were more highly up-regulated in TC roots than in YQ roots. Two genes in the YSL family (*YSL1-3* and *YSL1-1*) were markedly up-regulated in YQ leaves at 24 HAC, and *YSL1-2* transcript levels were high in TC leaves at 0 HAC. In all, although most of the transport genes were up-regulated in both cultivar roots, the specific DEGs with different expression profiles between TC and YQ in response to Cd may be related to the differences in Cd translocation efficiency between the two cultivars.

Cd-induced reduction of a chloroplast RNA fragment

We performed small RNA sequencing on the same samples to determine the responses of small RNAs to Cd stress (Table S6). Reads that mapped to the genomes (nuclear, mitochondrial and chloroplast) showed a minor 21 nt peak and a major 24 nt peak in all samples, consistent with observations in *Arabidopsis* (Li et al. 2016). Surprisingly, the leaf samples had a peak at 22 nt, and the 22 nt peak was reduced in YQ leaves at 24 HAC and 48 HAC and reduced in TC leaves at 48 HAC (Fig. S5).

Mapping the 22 nt sRNAs to genomic features revealed that nearly half of them were derived from unannotated regions (designated as the “others” category), and the percentage of sRNAs in the “others” category was obviously reduced under Cd stress (Fig. 4a). Further analysis revealed that the “others” category was largely composed of a single sRNA (AGTTACTAATTCATGATCTGGC) located in the 5’ UTR of two identical chloroplast genes (*ndhB.1 / ndhB.2*), so we henceforth refer to it as *ndhB* sRNA (Fig. 4b). The abundance of this sRNA was reduced by Cd stress in the leaves of both TC and YQ, but the decrease was more rapid in YQ (Fig. 4c). RNA gel blot analysis gave consistent results with the sRNA-seq data (Fig. 4d). The *ndhB* sRNA was also found in *Arabidopsis thaliana* at high abundance, and it was proposed to be a ‘footprint’ of the pentatricopeptide repeat (PPR) protein CRR2 (Ruwe and Schmitz-Linneweber 2012; Ruwe et al. 2016). We did not detect differential expression of *CRR2* under Cd stress in RNA-seq (Fig. S6). Among the surrounding genes of this 22 nt sRNA, *rps12*, *rps7* and *ndhB* belong to one precursor RNA (Hildebrand et al. 1988). RT-qPCR analysis showed that *ndhB* was down-regulated in YQ leaves at 24 and 48 HAC as well as in TC leaves at 48 HAC, while the levels of *rps7* or *rps12* transcripts were minimally affected when comparing to *ndhB* (Fig. 4e). Therefore, Cd stress reduced the abundance of the *ndhB* sRNA and, in YQ leaves with higher levels of Cd accumulation (Fig. 1b), also down-regulated the expression of the NADH oxidoreductase genes *ndhB.1* / *ndhB.2* in leaves.

PPR proteins are encoded in the nucleus but regulate gene expression in mitochondria and chloroplasts in post-transcriptional processes including splicing, RNA maturation, RNA editing and translation (Manna 2015; Cheng et al. 2016b). PPR proteins are RNA-binding proteins that recognize and bind to specific sequences in organellar RNAs (Shikanai and Fujii 2013). The regions bound by PPR proteins are protected from degradation and are found in the small RNA transcriptome (Ruwe et al. 2016). Thus, the *ndhB* sRNA is a footprint of CRR2 on *ndhB* transcripts. CRR2 is important for the maturation of the *nhdB* transcript from the polycistronic RNA *rps12-rps7-ndhB* transcript (Hashimoto et al. 2003). Loss of function of *CRR2* results in the absence of *nhdB* RNA without much effects on the accumulation of the *rps12-rps7* transcript (Hashimoto et al. 2003). The reduction in *ndhB* RNA levels by Cd treatment but not those of *rps12* or *rps7*, together with the reduction in the levels of the 22 nt *ndhB* sRNA, suggests that CRR2-mediated *ndhB* RNA maturation is compromised by Cd stress.

To determine how whether Cd stress might re-program organellar gene expression through nuclear *PPR* genes in general, we examined the expression profiles of *PPR* family genes in RNA-seq. Strikingly, 61 and 108 *PPR* family genes were differentially regulated after Cd stress in TC and YQ leaves, respectively, and nearly all of them were down-regulated at 24 HAC. Perhaps, this suggests that Cd stress led to a compromise in the nuclear control of organellar gene expression. The expression of many *PPR* genes recovered or even became up-regulated at 48 HAC, indicating a recovery of nucleus-mediated regulation

of organellar gene expression. Between YQ and TC, more *PPR* genes were down-regulated at 24 HAC in YQ, and less recovery of *PPR* expression was observed at 48 HAC (Fig. 4f), indicating a more severe Cd stress response in YQ leaves.

Differentially expressed miRNAs (DEMs) and their targets in response to Cd stress

As described above, the third most abundant sRNA class by length was the 21 nt sRNA class (Fig. S5), of which 22%-36% were miRNAs (Fig S7). Except in YQ roots, the percentage of 21 nt reads mapping to miRNA regions increased at 48 HAC (Fig S7), which may be correlated with the up-regulation of specific 21 nt miRNAs, including bra-miR397-3p, bra-miR397-5p and bra-miR398-3p (Table S7).

Because the miRNA annotations we used were from 2015 (Sun et al. 2015) and the criteria for plant miRNAs were recently revised by Axtell & Meyers (2018), we performed miRNA discovery with our sRNA-seq data using ShortStack (Axtell 2013) according to the new criteria for plant miRNA annotation. The analysis identified 112 annotated *MIR* loci meeting the new criteria in at least two independent libraries, and they accounted for approximately 17% of the annotated miRNAs from 2015 (Sun et al. 2015) (Fig. S8a). Moreover, we identified four new members of known *MIR* gene families, *bra-MIR6028c*, *bra-MIR403b*, *bra-MIR6030* and *bra-MIR171f* (Fig. S8b). We also identified three novel *MIR* loci that do not belong to known *MIR* gene families in miRbase (Fig. S8c). These new *MIR* family members or novel *MIR* loci had the potential to form pre-miRNAs with stem-loop structures. In addition, miRNA-5p and miRNA-3p sequences from these loci were both detected in our sRNA-seq and together accounted for more than 75% of the reads from the loci (Fig. S8b and c).

As our sRNA-seq only included the leaves and roots of young seedlings and may thus miss miRNAs of low abundance in our annotation, all annotated miRNAs (Sun et al. 2015) were used for analysis of differentially expressed miRNAs (DEMs). Except for the leaf samples at 24 HAC, numbers of DEMs were similar between TC and YQ after Cd stress (Fig. S9a). There were more DEMs in roots than in leaves, and the number of overlapping DEMs between TC and YQ was also more in roots than in leaves (Fig. S9b). There were more specific DEMs in YQ leaves at 24 HAC, and this feature was similar to the abundant specific DEGs in YQ leaves at 24 HAC (Fig. S2c), which implied that Cd stress also exerted more evident impact in YQ leaves than TC leaves on miRNAs. We also performed the DEM analysis with only the *MIR* loci meeting the new criteria. Most of the DEMs were conserved miRNAs (e.g., bra-miR156, bra-miR397 and bra-miR398), but still some non-conserved miRNAs were differentially expressed in response to Cd (Fig. 5 and Fig. 6). For example, bra-miR9560.2-5p (24 nt) was significantly up-regulated in roots and leaves of the two cultivars, and bra-miR5718-3p (22 nt) and bra-miR6202-5p (21 nt) were significantly down-regulated in both TC and YQ roots (Fig. 5 and Fig. 6). Bra-miR403b-3p and -5p from the newly identified *MIR403* family member, were identified as up-regulated DEMs in YQ leaves upon Cd stress at 24 HAC, indicating that these non-conserved miRNAs are probably early response factors to Cd stress.

To further confirm the potential function of DEMs in downstream regulation, tissue-specific degradome sequencing (degradome-seq) was performed on the leaves and roots with equally mixed RNA from samples of 0, 24 and 48 HAC. A total of 199 and 203 degradome target sites were detected respectively in

leaves and roots and their potential corresponding trigger miRNAs were listed in Table S8. The DEMs with corresponding targets detected in degradome-seq were also marked in Fig. 5 and Fig. 6. As the results showed, bra-miR162-3p, bra-miR171-3p and bra-miR396-5p were DEMs in leaves with confirmed targets and bra-miR156-5p, bra-miR156g-5p, bra-miR159-3p, bra-miR160-5p, bra-miR162-3p, bra-miR166-3p, bra-miR169-5p, bra-miR171-3p, bra-miR395-3p, bra-miR396-5p, bra-miR397-5p, bra-miR398-3p, and bra-miR6090-3p were DEMs in roots with confirmed targets. These 16 miRNAs likely play regulatory roles in Cd stress response.

The levels of miRNAs in *B. parachinensis* seedlings treated by Cd stress were further verified by RNA gel blot analysis (Fig. 7a and b). Results showed that bra-miR398-3p was strongly up-regulated in leaves and roots under Cd treatment. Cd stress also up-regulated bra-miR397-5p and down-regulated bra-miR156-5p in TC and YQ roots. In leaves, bra-miR171-3p and bra-miR396-5p were down-regulated by Cd stress and the down-regulation was partially recovered in TC at 48 HAC. The expression profiles of the target genes of the verified miRNAs had changes in the opposite direction compared to their corresponding miRNAs (Fig. 7c and d). Among them, the target genes of bra-miR398-3p, which encode mavicyanin-like proteins, were obviously down-regulated in both TC and YQ. Laccase (LAC) family members, *LAC11-1* and *LAC4-2*, which are targeted by bra-miR397-5p, were significantly down-regulated in YQ roots and slightly down-regulated in TC roots. Three target genes of bra-miR171-3p, encoding the scarecrow-like protein (SCL) family members, were significantly up-regulated in YQ leaves at 24 HAC and in TC leaves at 48 HAC. Although the target genes of bra-miR156-5p, encoding the SQUAMOSA promoter binding protein-like (SPL) family members, were not identified as DEGs except for *SPL9*, their transcript levels showed an upward trend under Cd treatment. Regarding the targets of bra-miR396-5p, only one of them was identified as a DEG (BraA01003773, which encodes beta-glucosidase 44, BGL44), and it was down-regulated in YQ leaves at 48 HAC. Degradome target-plots (T-plots) further showed that the above-mentioned miRNA target DEGs exhibited a unique and high peak corresponding to the predicted miRNA cleavage site (Fig. S10), thus verifying miRNA-guided cleavage.

To summarize, many miRNAs in *B. parachinensis* were differentially expressed in response to Cd stress. In particular, bra-miR156-5p, bra-miR398-3p, bra-miR397-5p and bra-miR171-3p were shown to regulate their target genes in response to Cd stress via RNA-seq and degradome sequencing.

Discussion

Metal ion transporters and Cd accumulation

Cd is a non-essential element for, and toxic to, plants (Lin and Aarts 2012). However, Cd may occupy the transport channels for other essential metal elements such as iron, zinc and copper because of their similar chemical properties (Sarwar et al. 2010). When *B. parachinensis* was treated with a high concentration of Cd, some transport-related genes, including metal ion transport genes and transmembrane transport genes, were up-regulated in the two tested cultivars (Fig. 3). Our findings

suggest that the up-regulation of metal ion transport related genes is a common response in the two cultivars and may even be a common response in *B. parachinensis.* In *B. napus*, Cd stress similarly up-regulates transport-related genes (Zhang et al. 2018b). Up-regulation of these transporters may lead to the non-selective, competitive absorption and transportation of both Cd^{2+} and other metal ions and increase Cd accumulation in plants. This model is consistent with the observation that the application of trace element fertilizers can reduce Cd accumulation in plants, which has been proposed as a strategy for the prevention and control of Cd pollution (Sarwar et al. 2010). Thus, blindly mutating individual transporter genes would be a misguided strategy to reduce Cd accumulation in plants. Instead, Cd-specific transporters or specific transporter domains that confer Cd selectivity should be identified and targeted for the breeding of crops with low Cd accumulation.

While many metal transporter genes are commonly up-regulated upon Cd stress in the two cultivars, some show different expression profiles. These may help to understand the differential Cd transport efficiencies between the two cultivars. Six genes in the ABCC family (*ABCC3-3*, *ABCC3-1*, *ABCC1-2*, *ABCC15*, *ABCC4-1* and *ABCC7*) were up-regulated at 24 HAC in YQ leaves but not in TC leaves (Fig. 3). As some members of the ABCC family (e.g., *Arabidopsis ABCC3*, *ABCC1* and *ABCC2*) serve as transporters of phytochelatin-Cd complexes (Brunetti et al. 2015), the up-regulation of these six ABCC family genes may reflect an increase in the transport of the phytochelatin-Cd complexes in YQ leaves (Fig. 8a). A similar phenomenon was also observed for YSL family genes. It was reported that maize YSL1 transports nicotianamine-metal complexes, and could transport Cd at a low rate (Schaaf et al. 2004). Two YSL family genes, *YSL1-3* and *YSL1-1*, were markedly up-regulated in YQ leaves at 24 HAC, which may increase Cd transport in YQ leaves (Fig. 8a). It was reported that some HMA family genes that are specifically expressed in roots (e.g., rice *HMA3*) are involved in the sequestration of Cd in vacuoles in root cells (Ueno et al. 2010). We found that two HMA family genes, *HMA2-1* and *HMA3*, were more highly up-regulated in TC roots than in YQ roots. These two genes may contribute to the lower root-to-shoot Cd translocation efficiency in TC (Fig. 8a).

Due to the different Cd translocation efficiency, the number of DEGs in leaves was larger in the YQ cultivar. The expression profiles also showed that most of the Cd-responsive DEGs, especially those related to basal metabolism, signaling and stimulus response, maintained their expression changes in YQ for a longer time, while most DEGs in TC recovered their normal expression levels at 48 HAC. In addition, some chloroplast genes and *PPR* genes, which are in the nuclear genome but regulate gene expression in mitochondria and chloroplasts (Manna 2015; Cheng et al. 2016b), were also affected by Cd to a larger extent in YQ leaves (Fig. 4). These findings indicate that, as compared to TC, YQ exhibits a more extensive and lasting response to Cd stress in leaves.

PPR genes involved in Cd response in *B. parachinensis*

To our knowledge, an sRNA peak at 22 nt in leaves has never been observed in sRNA-seq studies of other *Brassica* species, including *B. rapa* ssp. *pekinensis* cv. *Chiifu* (Kim et al. 2012; Sun et al. 2015), *B. parachinensis* (Zhou et al. 2017) and *B. napus* (Jian et al. 2018), and 22 nt sRNAs were not examined in

previous sRNA-seq studies of Cd stress responses in plants (Han et al. 2016; Kang et al. 2017; Jian et al. 2018). In the present study, we found a 22 nt *ndhB* sRNA showing a Cd-induced decrease in abundance in leaves of both *B. parachinensis* cultivars (Fig. 4). The *ndhB* sRNA reduction probably reflects reduced maturation of the *ndhB* transcript from the polycistronic precursor *rps12-rps7-ndhB* by Cd stress. The *PPR* gene *CRR2* encodes an RNA-binding protein that specifically associates with the *rps12-rps7-ndhB* RNA through the 22-nt sequence and promotes *ndhB* maturation from the polycistronic precursor RNA (Hashimoto et al. 2003; Ruwe and Schmitz-Linneweber 2012). In *crr2* mutants, abundance of the mature *ndhB* transcript is drastically reduced but that of *rps12-rps7* is unaffected (Hashimoto et al. 2003). We found that Cd stress had a similar effect on the transcripts from the polycistronic precursor as *crr2* mutations, suggesting that CRR2's ability to process the polycistronic transcript is compromised by Cd stress (Fig. 8a). While *CRR2* expression was not affected by Cd at the transcript level, the reduction in the CRR2 footprint (the 22 nt sRNA) implies that either CRR2 protein level were reduced or the binding of CRR2 to *ndhB* RNA was compromised by Cd.

PPR proteins are important regulators of RNA editing, maturation, stabilization or intron splicing in chloroplasts and mitochondria (Manna 2015; Cheng et al. 2016b). Strikingly, we found that many *PPR* genes were down-regulated upon Cd stress in both cultivars. This implies that Cd exerts a broad effect on organellar gene expression at the post-transcriptional level. We observed that Cd stress had a stronger effect on the expression of some chloroplast genes and nuclear *PPR* genes in the cultivar with higher Cd translocation efficiency (Fig. 4e and 4f). The expression of most of down-regulated *PPR* genes recovered in the cultivar with lower Cd accumulation, but not in the cultivar with higher Cd accumulation. The lasting and strong suppression of *PPR* genes in the cultivar with higher Cd accumulation further corroborates the hypothesis that Cd compromises the nuclear control of chloroplast genes.

Correlation between miRNAs and targets in *B. parachinensis* Cd response

Many miRNAs responsive to Cd stress have been identified in different species by high-throughput sequencing (Zhou et al. 2012b; Fang et al. 2013; Han et al. 2016; Jian et al. 2018). In the present study, Cd stress responsive miRNAs were identified based on exhaustive miRNA annotation and an improved mapping strategy (Fig. 5 and Fig. 6). The identified miRNAs included the novel miRNAs bra-miR6028c-3p, bra-miR403b-3p and -5p as well as non-conserved miRNAs, including bra-miR9560-5p, bra-miR1140-5p, bra-miR6090-3p, bra-miR5718-3p and bra-miR6202-5p. Among them, bra-miR6090-3p also had a degradome-seq confirmed target, BraA06002605, which encodes a GDSL esterase (Fig. S10). These miRNAs may be specific to some families/species or expressed only under cadmium stress.

A number of conserved miRNAs were also identified as DEMs. Among them, bra-miR156-5p, bra-miR171-3p and bra-miR396-5p under Cd stress, were consistent with previous findings in rice from microarray analysis (Ding et al. 2011). However, the expression of these conserved miRNAs was not affected by Cd stress in previous sRNA-seq studies of rapeseed (Zhou et al. 2012a) or *B. parachinensis* (Zhou et al. 2017). In the present study, the differential expression of these miRNAs was verified by RNA gel blot analysis and their confirmed target genes were correspondingly affected.

It is noteworthy that Cd stress led to significant up-regulation of both bra-miR397-5p and bra-miR398-3p and significant down-regulation of their target genes, *LAC4-2/11-1* and a mavicyanin-like protein gene, respectively. These changes are similar to the findings in *Arabidopsis thaliana* (Gielen et al. 2016), and these two miRNAs have also been implicated in copper homeostasis regulation (Ding and Zhu 2009). It has been found that *SPL7* and phytochelatin synthase induce miR397 and miR398 levels after Cd stress (Gielen et al. 2016, 2017). A possible mechanism of phytochelatin-mediated induction of miR398 is that Cd increases the levels of phytochelatins, which then chelate both Cd and Cu to induce cellular Cu deficiency; and the increase in miR398 is a well-known Cu deficiency response (Gielen et al. 2016, 2017). It is also known that *MIR397* and *MIR398* expression is regulated by SPL7 through promoter binding (Yamasaki et al. 2009). In this study, we found that bra-miR156-5p and its target *SPL* genes were down- and up-regulated, respectively, by Cd stress (Fig. 5). We therefore propose a regulatory pathway involving the following components: (Cd^{2+}/Cu^{2+}) - miR156 - *SPL7* - (miR397 / miR398) - (*LAC4-2/11-1* / mavicyanin-like protein gene) (Fig. 8b). Phytochelatin-mediated regulation of miR398 probably interfaces with this pathway to form a network of gene expression responsive to Cd stress.

In summary, in response to Cd stress, the expression of *B. parachinensis* genes related to metal ion transport and transmembrane transport significantly increased. The chloroplast gene *ndhB* and *PPR* genes were significantly reduced in expression by Cd stress. The differential severity of gene expression changes in the two cultivars was correlated to differences in their Cd translocation efficiency. Many miRNAs, including conserved and none-conserved, are likely involved in the initial response to Cd. Among them, miR156, miR397, miR398 and their target genes form a possible regulatory pathway in Cd stress response. These findings help better understand the mechanisms of Cd stress response in plants.

Declarations

Acknowledgements

We thank Chengjie Chen for his TBtools software. We thank Dr. Juan He, Dr. Xufeng Wang, Dr. Peng Tian and Dr. Wenwen Kong for their codes and advice for the data analysis. This work was supported by the Guangdong Innovation Research Team Fund (2014ZT05S078).

Author contributions

YT, XC and SL designed the experiments. SL and WZ performed the biomass, Cd content determination, RNA isolation and libraries construction. YL, CY, LG and XC performed the bioinformatics analysis. YL, SL

and YD performed the qRT-PCR and RNA gel blotting. YL wrote the manuscript. XC, YT and LG revised the manuscript.

Conflict of interest

The authors declare no conflict of interest.

References

Addo-Quaye C, Miller W, Axtell MJ (2009) CleaveLand: A pipeline for using degradome data to find cleaved small RNA targets. Bioinformatics 25:130–131. https://doi.org/10.1093/bioinformatics/btn604

Axtell MJ (2013) ShortStack: Comprehensive annotation and quantification of small RNA genes. RNA 19:740–751. https://doi.org/10.1261/rna.035279.112

Axtell MJ, Meyers BC (2018) Revisiting criteria for plant microRNA annotation in the era of big data. Plant Cell 30:272–284. https://doi.org/10.1105/tpc.17.00851

Bairoch A, Apweiler R (2000) The SWISS-PROT protein sequence database and its supplement TrEMBL in 2000. Nucleic Acids Res 28:45–48

Brunetti P, Zanella L, De Paolis A, et al (2015) Cadmium-inducible expression of the ABC-type transporter AtABCC3 increases phytochelatin-mediated cadmium tolerance in *Arabidopsis*. J Exp Bot 66:3815–3829. https://doi.org/10.1093/jxb/erv185

Cai C, Wang X, Liu B, et al (2017) *Brassica rapa* genome 2.0: A reference upgrade through sequence re-assembly and gene re-annotation. Mol Plant 10:649–651. https://doi.org/10.1016/j.molp.2016.11.008

Camacho C, Coulouris G, Avagyan V, et al (2009) BLAST+: architecture and applications. BMC Bioinformatics 10:421. https://doi.org/10.1186/1471-2105-10-421

Chen C, Chen H, He Y, Xia R (2018) TBtools,a Toolkit for Biologists integrating various biological data handling tools with a user-friendly interface. bioRxiv 289660. https://doi.org/10.1101/289660

Chen Y, Zhi J, Zhang H, et al (2017) Transcriptome analysis of *Phytolacca americana* L. in response to cadmium stress. PLoS One 12:e0184681. https://doi.org/10.1371/journal.pone.0184681

Cheng F, Sun R, Hou X, et al (2016a) Subgenome parallel selection is associated with morphotype diversification and convergent crop domestication in *Brassica rapa* and *Brassica oleracea*. Nat Genet 48:1218–1224. https://doi.org/10.1038/ng.3634

Cheng S, Gutmann B, Zhong X, et al (2016b) Redefining the structural motifs that determine RNA binding and RNA editing by pentatricopeptide repeat proteins in land plants. Plant J 85:532–547.

https://doi.org/10.1111/tpj.13121

Ding Y, Chen Z, Zhu C (2011) Microarray-based analysis of cadmium-responsive microRNAs in rice (*Oryza sativa*). J Exp Bot 62:3563–3573. https://doi.org/10.1093/jxb/err046

Ding Y, Gong S, Wang Y, et al (2018) MicroRNA166 modulates cadmium tolerance and accumulation in rice. Plant Physiol 177:1691–1703. https://doi.org/10.1104/pp.18.00485

Ding YF, Zhu C (2009) The role of microRNAs in copper and cadmium homeostasis. Biochem Biophys Res Commun 386:6–10. https://doi.org/10.1016/j.bbrc.2009.05.137

Dobin A, Davis CA, Schlesinger F, et al (2013) STAR: ultrafast universal RNA-seq aligner. Bioinformatics 29:15–21. https://doi.org/10.1093/bioinformatics/bts635

Ernst J, Bar-Joseph Z (2006) STEM: A tool for the analysis of short time series gene expression data. BMC Bioinformatics 7:1–11. https://doi.org/10.1186/1471-2105-7-191

Fang X, Zhao Y, Ma Q, et al (2013) Identification and comparative analysis of cadmium tolerance-associated miRNAs and their targets in two soybean genotypes. PLoS One 8:e81471. https://doi.org/10.1371/journal.pone.0081471

Feng J, Jia W, Lv S, et al (2018) Comparative transcriptome combined with morpho-physiological analyses revealed key factors for differential cadmium accumulation in two contrasting sweet sorghum genotypes. Plant Biotechnol J 16:558–571. https://doi.org/10.1111/pbi.12795

Gao J, Sun L, Yang X, Liu JX (2013) Transcriptomic analysis of cadmium stress response in the heavy metal hyperaccumulator *Sedum alfredii* Hance. PLoS One 8:e64643. https://doi.org/10.1371/journal.pone.0064643

Gielen H, Remans T, Vangronsveld J, Cuypers A (2016) Toxicity responses of Cu and Cd: The involvement of miRNAs and the transcription factor SPL7. BMC Plant Biol 16:1–16. https://doi.org/10.1186/s12870-016-0830-4

Gielen H, Vangronsveld J, Cuypers A (2017) Cd-induced Cu deficiency responses in *Arabidopsis thaliana*: are phytochelatins involved? Plant Cell Environ 40:390–400. https://doi.org/10.1111/pce.12876

Han X, Yin H, Song X, et al (2016) Integration of small RNAs, degradome and transcriptome sequencing in hyperaccumulator Sedum alfredii uncovers a complex regulatory network and provides insights into cadmium phytoremediation. Plant Biotechnol J 14:1470–1483. https://doi.org/10.1111/pbi.12512

Hashimoto M, Endo T, Peltier G, et al (2003) A nucleus-encoded factor, CRR2, is essential for the expression of chloroplast *ndhB* in *Arabidopsis*. Plant J 36:541–549. https://doi.org/10.1046/j.1365-313X.2003.01900.x

Hildebrand M, Hallick RB, Passavant CW, Bourque DP (1988) Trans-splicing in chloroplasts: the *rps12* loci of *Nicotiana tabacum*. Proc Natl Acad Sci 85:372–376. https://doi.org/10.1073/pnas.85.2.372

Huang Y, He C, Shen C, et al (2017) Toxicity of cadmium and its health risks from leafy vegetable consumption. Food Funct 8:1373–1401. https://doi.org/10.1039/c6fo01580h

Jia T, Zhang B, You C, et al (2017) The *Arabidopsis* MOS4-associated complex promotes microRNA biogenesis and precursor messenger RNA splicing. Plant Cell 29:2626–2643. https://doi.org/10.1105/tpc.17.00370

Jian H, Yang B, Zhang A, et al (2018) Genome-wide identification of microRNAs in response to cadmium stress in oilseed rape (*Brassica napus* L.) Using High-Throughput Sequencing. Int J Mol Sci 19:1431. https://doi.org/10.3390/ijms19051431

Kang XP, Gao JP, Zhao JJ, et al (2017) Identification of cadmium-responsive microRNAs in *Solanum torvum* by high-throughput sequencing. Russ J Plant Physiol 64:283–300. https://doi.org/10.1134/S1021443717020066

Khan KY, Ali B, Cui X, et al (2017) Effect of humic acid amendment on cadmium bioavailability and accumulation by pak choi (*Brassica rapa ssp. chinensis* L.) to alleviate dietary toxicity risk. Arch Agron Soil Sci 63:1431–1442. https://doi.org/10.1080/03650340.2017.1283018

Kim B, Yu H-J, Park S-G, et al (2012) Identification and profiling of novel microRNAs in the *Brassica rapa* genome based on small RNA deep sequencing. BMC Plant Biol 12:218. https://doi.org/10.1186/1471-2229-12-218

Li S, Le B, Ma X, et al (2016) Biogenesis of phased siRNAs on membrane-bound polysomes in *Arabidopsis*. Elife 5:1–24. https://doi.org/10.7554/eLife.22750

Lin YF, Aarts MGM (2012) The molecular mechanism of zinc and cadmium stress response in plants. Cell Mol Life Sci 69:3187–3206. https://doi.org/10.1007/s00018-012-1089-z

Liu H, Zhao H, Wu L, et al (2017) Heavy metal ATPase 3 (HMA3) confers cadmium hypertolerance on the cadmium/zinc hyperaccumulator *Sedum plumbizincicola*. New Phytol 215:687–698. https://doi.org/10.1111/nph.14622

Love MI, Huber W, Anders S (2014) Moderated estimation of fold change and dispersion for RNA-seq data with DESeq2. Genome Biol 15:550. https://doi.org/10.1186/s13059-014-0550-8

Manna S (2015) An overview of pentatricopeptide repeat proteins and their applications. Biochimie 113:93–99. https://doi.org/10.1016/j.biochi.2015.04.004

Martin M (2011) Cutadapt removes adapter sequences from high-throughput sequencing reads. EMBnet.journal 17:10. https://doi.org/10.14806/ej.17.1.200

McCarthy FM, Gresham CR, Buza TJ, et al (2011) AgBase: supporting functional modeling in agricultural organisms. Nucleic Acids Res 39:D497–D506. https://doi.org/10.1093/nar/gkq1115

Nakamura SI, Akiyama C, Sasaki T, et al (2008) Effect of cadmium on the chemical composition of xylem exudate from oilseed rape plants (*Brassica napus* L.). Soil Sci Plant Nutr 54:118–127. https://doi.org/10.1111/j.1747-0765.2007.00214.x

Pall GS, Hamilton AJ (2008) Improved northern blot method for enhanced detection of small RNA. Nat Protoc 3:1077–1084. https://doi.org/10.1038/nprot.2008.67

Qiu Q, Wang Y, Yang Z, et al (2011a) Responses of different Chinese flowering cabbage (*Brassica parachinensis* L.) cultivars to cadmium and lead exposure: screening for Cd + Pb pollution-safe cultivars. CLEAN - Soil, Air, Water 39:925–932. https://doi.org/10.1002/clen.201000275

Qiu Q, Wang Y, Yang Z, Yuan J (2011b) Effects of phosphorus supplied in soil on subcellular distribution and chemical forms of cadmium in two Chinese flowering cabbage (*Brassica parachinensis* L.) cultivars differing in cadmium accumulation. Food Chem Toxicol 49:2260–2267. https://doi.org/10.1016/j.fct.2011.06.024

Rizwan M, Ali S, Zia ur Rehman M, et al (2018) Cadmium phytoremediation potential of *Brassica* crop species: A review. Sci Total Environ 631–632:1175–1191. https://doi.org/10.1016/j.scitotenv.2018.03.104

Ruwe H, Schmitz-Linneweber C (2012) Short non-coding RNA fragments accumulating in chloroplasts: Footprints of RNA binding proteins? Nucleic Acids Res 40:3106–3116. https://doi.org/10.1093/nar/gkr1138

Ruwe H, Wang G, Gusewski S, Schmitz-Linneweber C (2016) Systematic analysis of plant mitochondrial and chloroplast small RNAs suggests organelle-specific mRNA stabilization mechanisms. Nucleic Acids Res 44:7406–7417. https://doi.org/10.1093/nar/gkw466

Sanità Di Toppi L, Gabbrielli R (1999) Response to cadmium in higher plants. Environ Exp Bot 41:105–130. https://doi.org/10.1016/S0098-8472(98)00058-6

Sarwar N, Saifullah, Malhi SS, et al (2010) Role of mineral nutrition in minimizing cadmium accumulation by plants. J Sci Food Agric 90:925–937. https://doi.org/10.1002/jsfa.3916

Sasaki A, Yamaji N, Ma JF (2014) Overexpression of *OsHMA3* enhances Cd tolerance and expression of Zn transporter genes in rice. J Exp Bot 65:6013–6021. https://doi.org/10.1093/jxb/eru340

Sasaki A, Yamaji N, Yokosho K, Ma JF (2012) Nramp5 is a major transporter responsible for manganese and cadmium uptake in rice. Plant Cell 24:2155–2167. https://doi.org/10.1105/tpc.112.096925

Schaaf G, Ludewig U, Erenoglu BE, et al (2004) ZmYS1 functions as a proton-coupled symporter for phytosiderophore- and nicotianamine-chelated metals. J Biol Chem 279:9091–9096. https://doi.org/10.1074/jbc.M311799200

Shikanai T, Fujii S (2013) Function of PPR proteins in plastid gene expression. RNA Biol 10:1446–1456. https://doi.org/10.4161/rna.25207

Shriram V, Kumar V, Devarumath RM, et al (2016) MicroRNAs as potential targets for abiotic stress tolerance in plants. Front Plant Sci 7:1–18. https://doi.org/10.3389/fpls.2016.00817

Sun C, Wu J, Liang J, et al (2015) Impacts of whole-genome triplication on *MIRNA* evolution in *Brassica rapa*. Genome Biol Evol 7:3085–3096. https://doi.org/10.1093/gbe/evv206

Supek F, Bošnjak M, Škunca N, Šmuc T (2011) REVIGO summarizes and visualizes long lists of gene ontology terms. PLoS One 6:e21800. https://doi.org/10.1371/journal.pone.0021800

Tang Z, Cai H, Li J, et al (2017) Allelic variation of *NtNramp5* associated with cultivar variation in cadmium accumulation in tobacco. Plant Cell Physiol 58:1583–1593. https://doi.org/10.1093/pcp/pcx087

Ueno D, Yamaji N, Kono I, et al (2010) Gene limiting cadmium accumulation in rice. Proc Natl Acad Sci 107:16500–16505. https://doi.org/10.1073/pnas.1005396107

Verret F, Gravot A, Auroy P, et al (2004) Overexpression of *AtHMA4* enhances root-to-shoot translocation of zinc and cadmium and plant metal tolerance. FEBS Lett 576:306–312. https://doi.org/10.1016/j.febslet.2004.09.023

Wang C, Cui H-M, Huang T-H, et al (2016) Identification and validation of reference genes for RT-qPCR analysis in non-heading chinese cabbage flowers. Front Plant Sci 7:1–12. https://doi.org/10.3389/fpls.2016.00811

Wang J, Yuan J, Yang Z, et al (2009) Variation in cadmium accumulation among 30 cultivars and cadmium subcellular distribution in 2 selected cultivars of water spinach (*Ipomoea aquatica* Forsk.). J Agric Food Chem 57:8942–8949. https://doi.org/10.1021/jf900812s

Wickham H (2016) ggplot2. Springer International Publishing, Cham

Wójcik M, Tukiendorf A (2011) Glutathione in adaptation of *Arabidopsis thaliana* to cadmium stress. Biol Plant 55:125–132. https://doi.org/10.1007/s10535-011-0017-7

Wu J, Liu B, Cheng F, et al (2012) Sequencing of Chloroplast Genome Using Whole Cellular DNA and Solexa Sequencing Technology. Front Plant Sci 3:1–7. https://doi.org/10.3389/fpls.2012.00243

Wu Z, Zhao X, Sun X, et al (2015) Xylem transport and gene expression play decisive roles in cadmium accumulation in shoots of two oilseed rape cultivars (*Brassica napus*). Chemosphere 119:1217–1223. https://doi.org/10.1016/j.chemosphere.2014.09.099

Xu H, Yu C, Xia X, et al (2018) Comparative transcriptome analysis of duckweed (*Landoltia punctata*) in response to cadmium provides insights into molecular mechanisms underlying hyperaccumulation. Chemosphere 190:154–165. https://doi.org/10.1016/j.chemosphere.2017.09.146

Yamasaki H, Hayashi M, Fukazawa M, et al (2009) SQUAMOSA promoter binding protein-like7 is a central regulator for copper homeostasis in *Arabidopsis*. PLANT CELL ONLINE 21:347–361. https://doi.org/10.1105/tpc.108.060137

Yao X, Cai Y, Yu D, Liang G (2018) bHLH104 confers tolerance to cadmium stress in *Arabidopsis thaliana*. J Integr Plant Biol 60:691–702. https://doi.org/10.1111/jipb.12658

Yu R, Tang Y, Liu C, et al (2017a) Comparative transcriptomic analysis reveals the roles of ROS scavenging genes in response to cadmium in two pak choi cultivars. Sci Rep 7:9217. https://doi.org/10.1038/s41598-017-09838-2

Yu Y, Jia T, Chen X (2017b) The 'how' and 'where' of plant microRNAs. New Phytol 216:1002–1017. https://doi.org/10.1111/nph.14834

Zhai J, Arikit S, Simon SA, et al (2014) Rapid construction of parallel analysis of RNA end (PARE) libraries for Illumina sequencing. Methods 67:84–90. https://doi.org/10.1016/j.ymeth.2013.06.025

Zhang J, Martinoia E, Lee Y (2018a) Vacuolar transporters for cadmium and arsenic in plants and their applications in phytoremediation and crop development. Plant Cell Physiol 59:1317–1325. https://doi.org/10.1093/pcp/pcy006

Zhang J, Zhang M, Shohag MJI, et al (2016) Enhanced expression of *SaHMA3* plays critical roles in Cd hyperaccumulation and hypertolerance in Cd hyperaccumulator *Sedum alfredii* Hance. Planta 243:577–589. https://doi.org/10.1007/s00425-015-2429-7

Zhang LW, Song JB, Shu XX, et al (2013) MiR395 is involved in detoxification of cadmium in *Brassica napus*. J Hazard Mater 250–251:204–211. https://doi.org/10.1016/j.jhazmat.2013.01.053

Zhang XD, Meng JG, Zhao KX, et al (2018b) Annotation and characterization of Cd-responsive metal transporter genes in rapeseed (*Brassica napus*). BioMetals 31:107–121. https://doi.org/10.1007/s10534-017-0072-4

Zhou Q, Yang Y-C, Shen C, et al (2017) Comparative analysis between low- and high-cadmium-accumulating cultivars of *Brassica parachinensis* to identify difference of cadmium-induced microRNA and their targets. Plant Soil 420:223–237. https://doi.org/10.1007/s11104-017-3380-0

Zhou ZS, Song JB, Yang ZM (2012a) Genome-wide identification of *Brassica napus* microRNAs and their targets in response to cadmium. J Exp Bot 63:4597–4613. https://doi.org/10.1093/jxb/ers136

Zhou ZS, Zeng HQ, Liu ZP, Yang ZM (2012b) Genome-wide identification of *Medicago truncatula* microRNAs and their targets reveals their differential regulation by heavy metal. Plant, Cell Environ 35:86–99. https://doi.org/10.1111/j.1365-3040.2011.02418.x

Figures

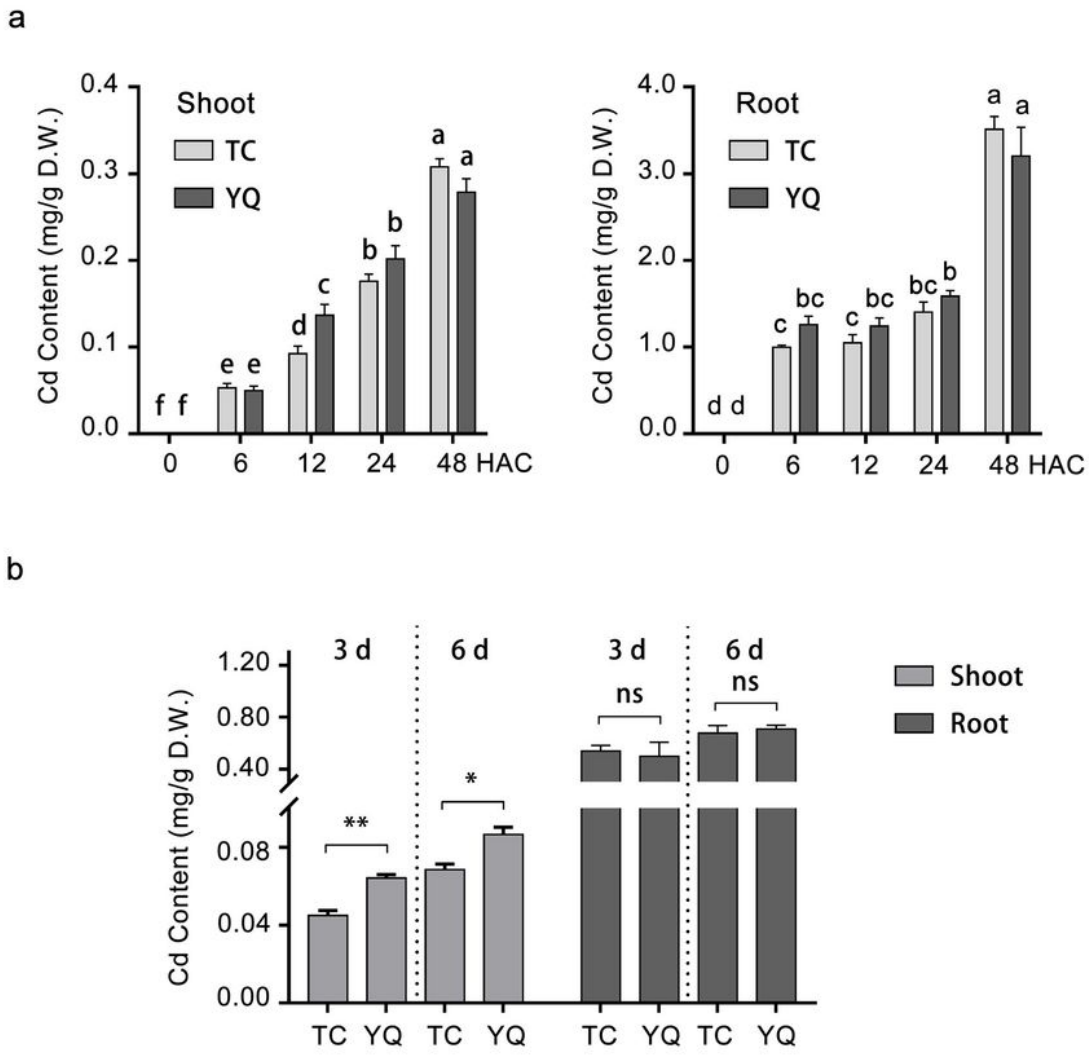

Figure 1

Cadmium (Cd) content in TC and YQ cultivars treated with different concentrations of Cd. TC and YQ, two cultivars of Brassica parachinensis; HAC, hours after Cd stress; D.W., dry weight. Fifteen-day-old hydroponic seedlings were treated with Cd, and their roots and shoots were harvested separately at different time points for Cd content determination. (a) Cd content in TC and YQ shoots and roots before and after 50 μM Cd treatment. Different lower-case letters indicate significant differences at $P < 0.05$

using Duncan's multiple range test. (b) Cd content in TC and YQ shoots and roots after 5 μM Cd treatment for 3 d and 6 d. Asterisks indicate significant differences between TC and YQ using a Student's t-test (*P < 0.05, **P < 0.01, ns: no significant difference).

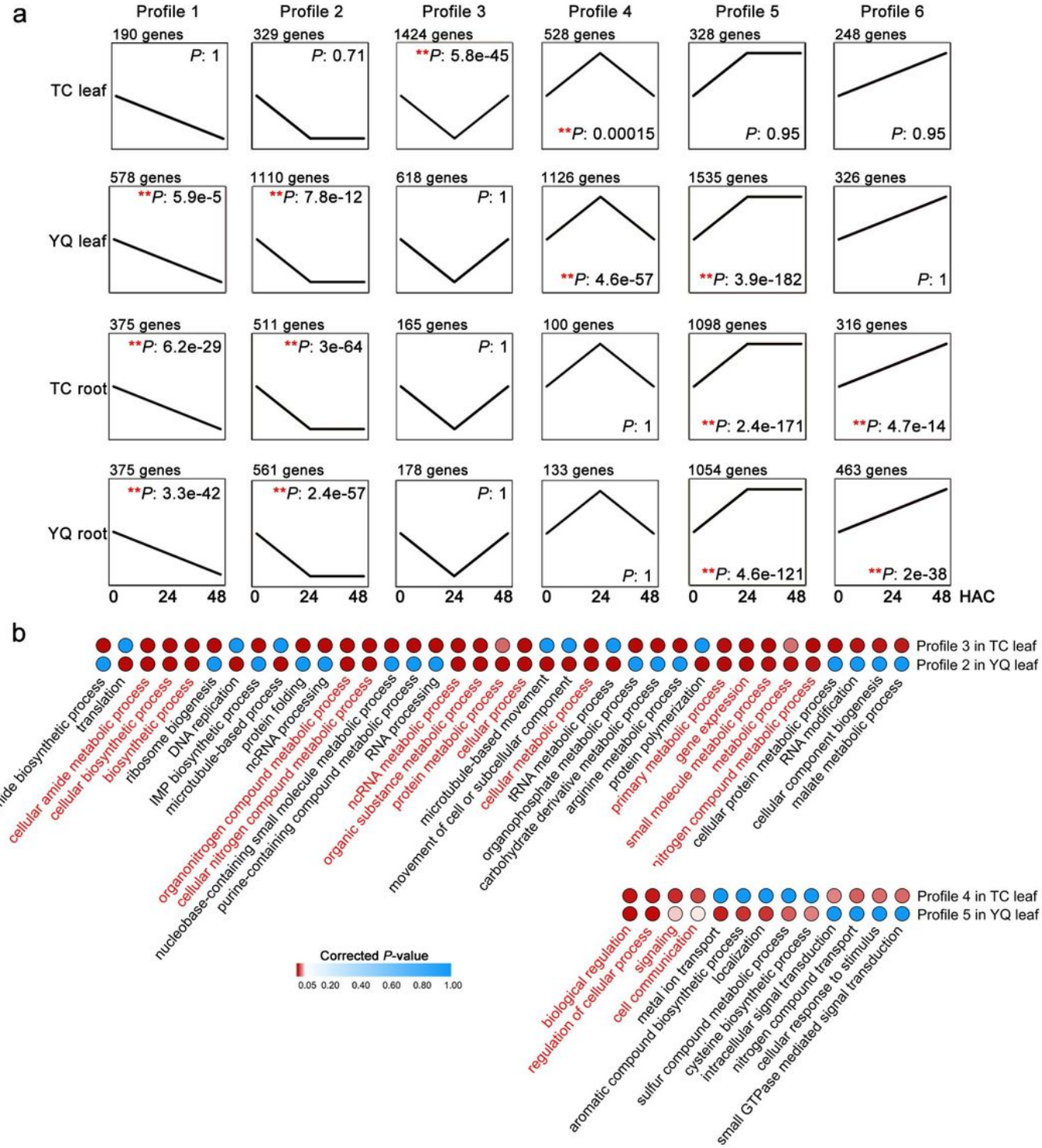

Figure 2

Temporal expression profiles and profile GO enrichment of TC and YQ under Cd stress. (a) Expression profiles of genes in response to Cd stress in TC and YQ leaves and roots. Gene number of a profile was

compared to the gene number of the profile from random assignment, and Bonferroni multiple hypothesis testing was used to evaluate the significance (**P < 0.01). (b) GO enrichment of the genes in the significant profiles (corrected P-value < 0.05, the Benjamini and Hochberg procedure was used to derive the corrected P-value.) in TC and YQ leaves. Different profiles in TC and YQ with similar GO terms are displayed. Only GO terms in the‘Biological Process’ category are shown in the figure, and redundant GO terms were removed by the online tool REVIGO. An entire list of enriched GO terms can be found in Table S3.

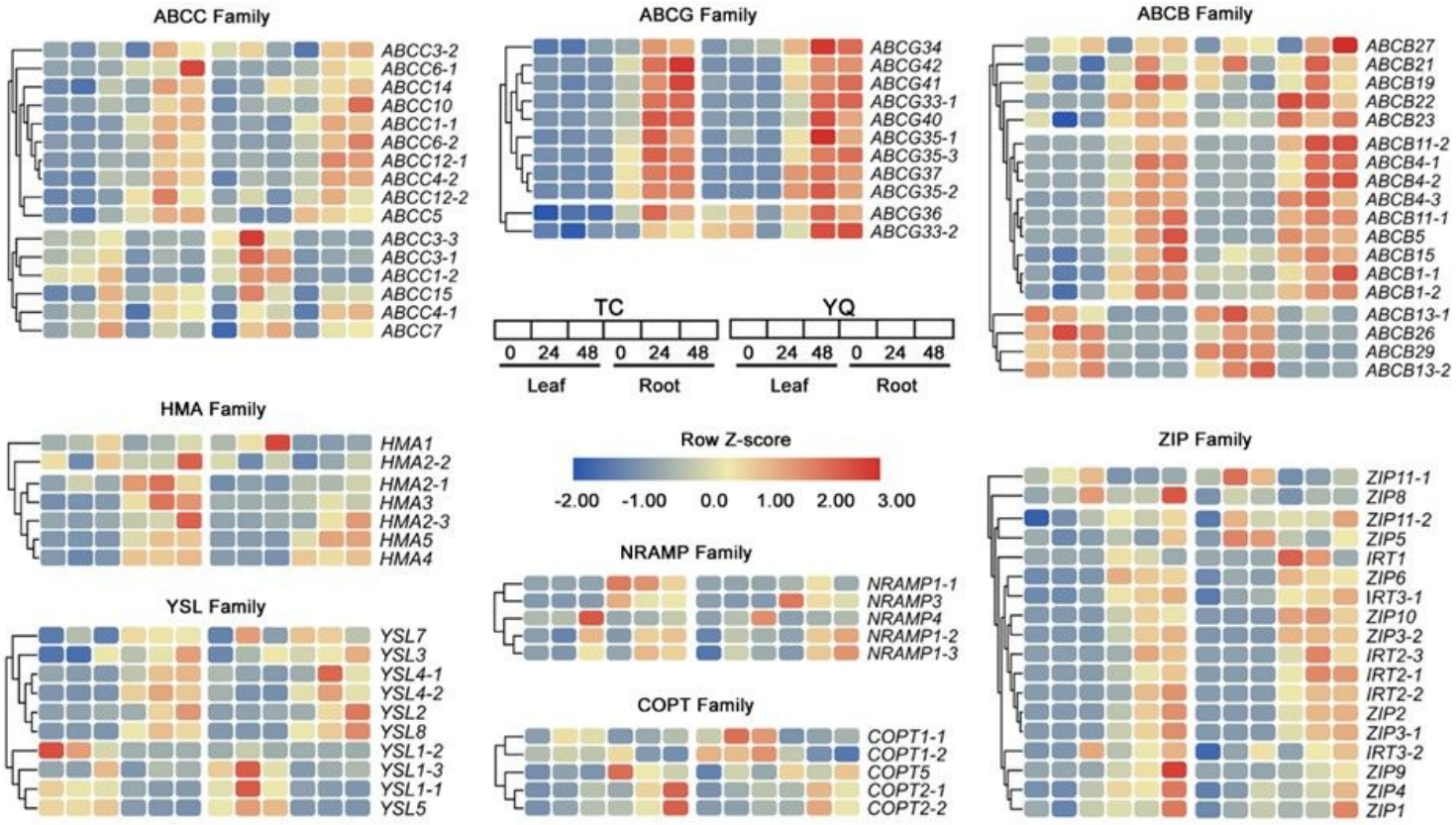

Figure 3

Expression profiles of DEGs related to metal ion transmembrane transport in response to Cd stress in YQ and TC. Red and blue indicate up- and down-regulation, respectively, and the TPM values were normalized by row. Refer to the diagram in the middle for the sample identity (cultivar, organ type, and time after Cd stress) of each column. ABCC, ATP-binding cassette transporter subfamily C protein; ABCG, ABC transporter subfamily G protein; ABCB, ABC transporter subfamily B protein; COPT, copper transporter; HMA, heavy-metal ATPase; ZIP, zinc/iron transporter; YSL, yellow stripe-like; NRAMP, natural resistance-associated macrophage protein.

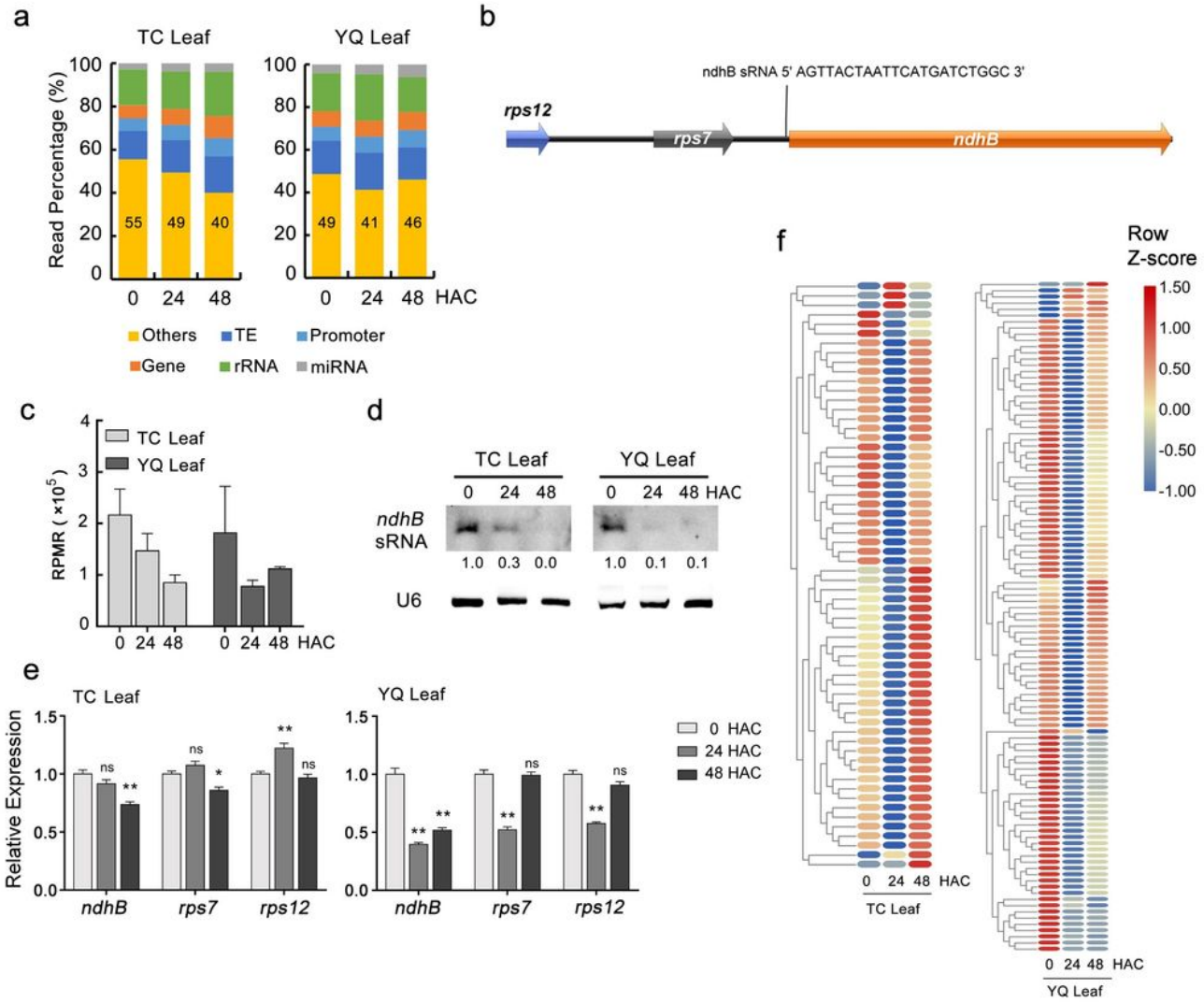

Figure 4

The reduction of a chloroplast sRNA in leaves after Cd stress. HAC, hours after Cd stress. (a) Distribution of genomic features that 22 nt sRNAs map to. TE, transposable element. Intergenic regions are included in the 'others' category. The numerical values in the "others" category indicate read percentage in this category. (b) Location of the major 22 nt sRNA (5' AGUUACUAAUUCAUGAUCUGGC 3') on the chloroplast genome. The small RNA maps to a region upstream of the ndhB gene. The three genes (rps12, rps7, and

ndhB) are in a polycistronic cluster. (c) Changes in abundance of the 22 nt sRNA in (b) in response to Cd stress as determined by sRNA-seq. RPMR, reads per million of 45S rRNA reads. (d) RNA gel blot analysis of the 22 nt sRNA in (b). U6 served as the loading control. The numbers represent relative abundance. (e) RT-qPCR analysis of three chloroplast genes located in a polycistronic cluster near the 22 nt sRNA in (b). Asterisks indicate significant differences between 0 HAC and 24 or 48 HAC using a Student's t-test (*P < 0.05, **P < 0.01, ns: no significant difference). (f) Expression profiles of pentatricopeptide repeat (PPR) genes that were found to be differentially expressed in RNA-seq from TC and YQ leaves in 24 HAC vs. 0 HAC or 48 HAC vs. 0 HAC.

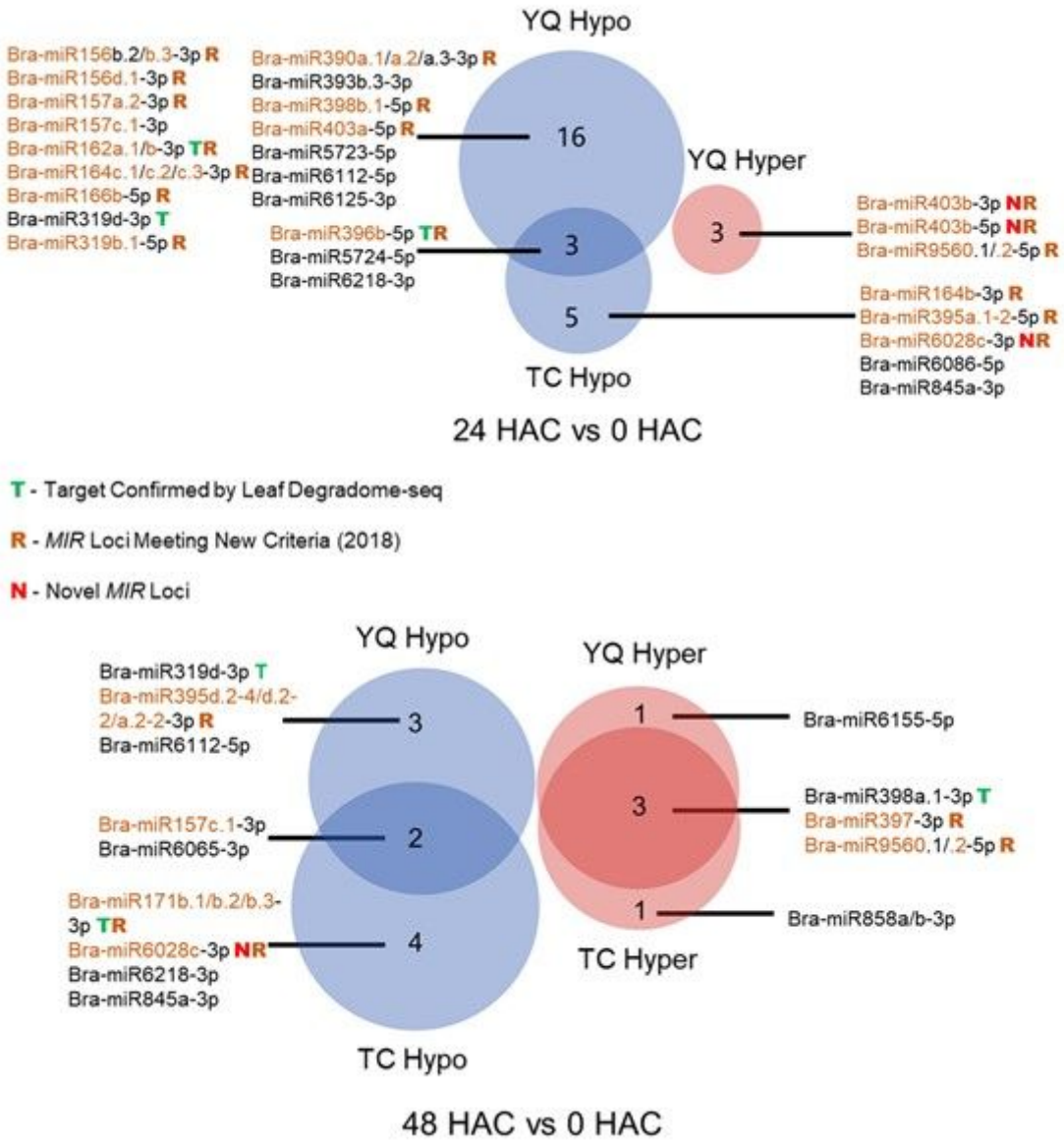

Figure 5

Differentially expressed miRNAs in YQ and TC leaves and their loci and target information. Brown text indicates MIR loci meeting the new criteria (Axtell and Meyers 2018), and they are also marked with a

brown, capital “R” following their names. MiRNAs whose targets were confirmed by degradome sequencing are marked with a green, capital “T” following their names. The red, capital “N” indicates miRNAs from the novel MIR loci.

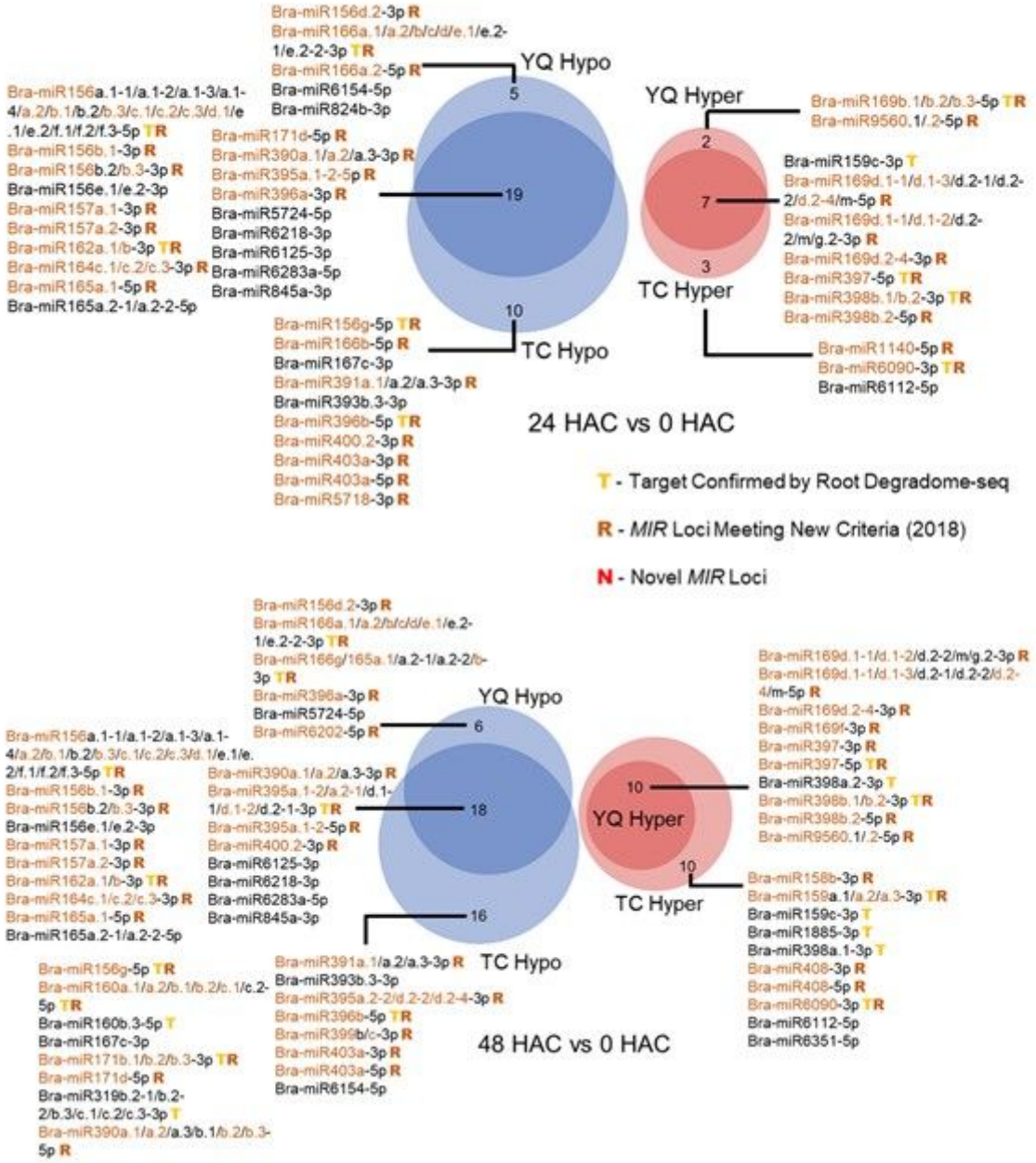

Figure 6

Differentially expressed miRNAs in YQ and TC roots and their loci and target information. Brown text indicates MIR loci meeting the new criteria (Axtell and Meyers 2018), and they are also marked with a brown, capital “R” following their names. MiRNAs whose targets were confirmed by degradome

sequencing are marked with a yellow, capital “T” following their names. The red, capital “N” indicates miRNAs from the novel MIR loci.

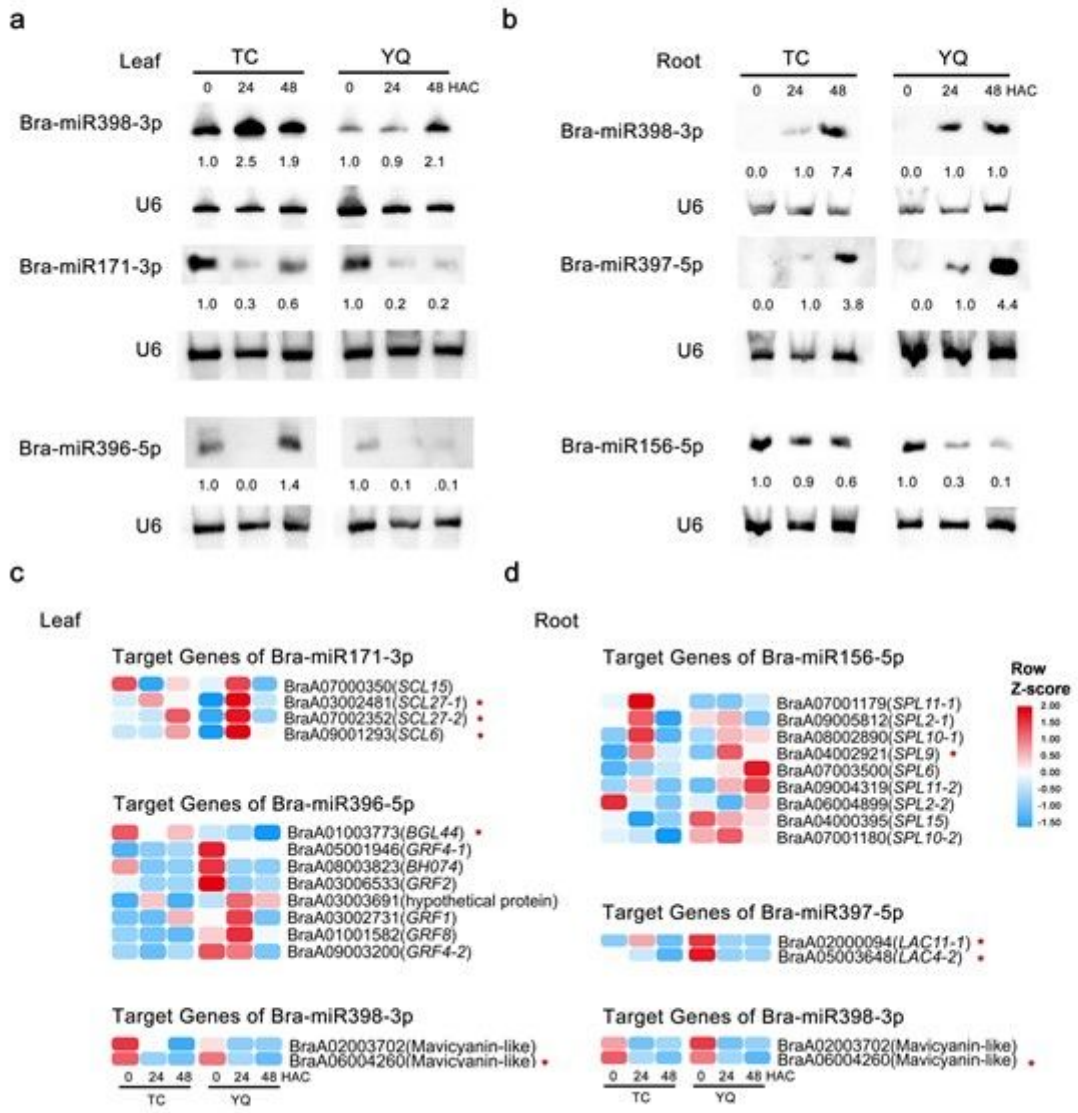

Figure 7

RNA gel blot verification of DEMs and expression profiles of their target genes. (a-b) RNA gel blot analysis of DEMs in leaf (a) and root (b). U6 served as the loading control. The numbers represent relative abundance. (c-d) Expression profiles of the target genes of the DEMs in (a) and (b) as determined by RNA-seq. All the target genes in (c) and (d) were verified by degradome sequencing. Red and blue color indicate up- and down-regulation, respectively, and the gene TPM (transcripts per million) values were normalized by row. Asterisks indicate genes identified as DEGs in roots or leaves at 24 or 48 HAC (hours after Cd stress) compared to 0 HAC. SPL, SQUAMOSA promoter-binding protein-like; SCL, scarecrow-like

protein; BGL44, beta-glucosidase 44; GRF, growth-regulating factor; BH074, transcription factor bHLH74. LAC, laccase.

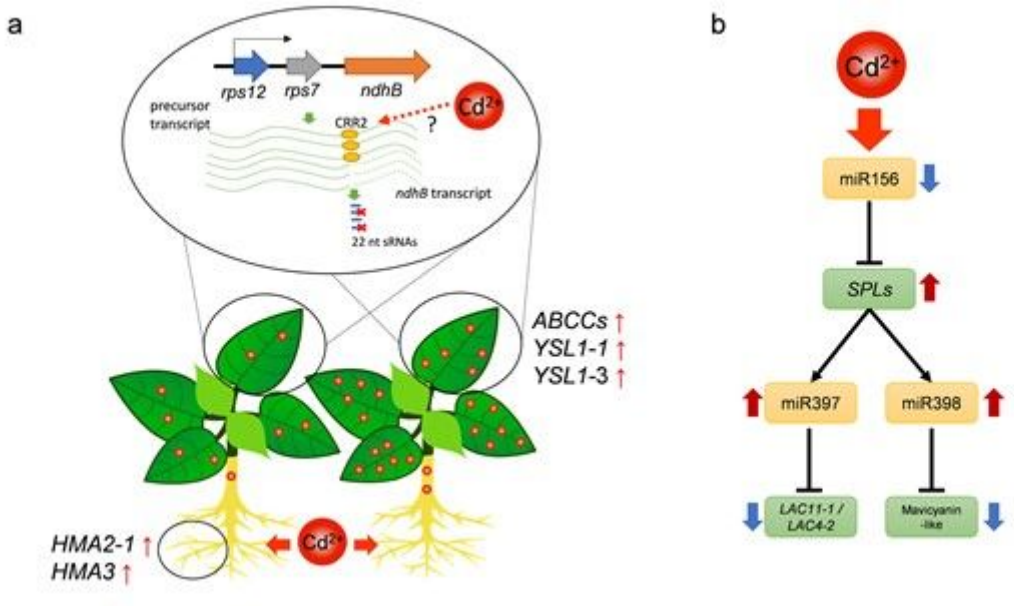

Figure 8

Proposed common or unique models of the cultivars with different Cd translocation efficiencies when responding to Cd stress. (a) Response of transporter genes and chloroplast-related genes after Cd stress in the cultivars with different Cd translocation efficiencies. In the cultivar with lower Cd translocation efficiency, HMA2-1 and HMA3 were both up-regulated in roots. In the cultivar with higher Cd translocation efficiency, some ABCC family genes and YSL1-1, YSL1-3 were both up-regulated in leaves. At the same time, when Cd reached the leaves, the function of a PPR protein CRR2 was affected for unknown reasons, and this resulted in the down-regulation of the ndhB transcript but not its precursor transcript. Further, the corresponding 22 nt small RNA were reduced after Cd stress. (b) A putative regulatory pathway of miRNAs and its target genes in Cd stress response. After Cd stress, miR156 were down-regulated and lead to the up-regulation of its target genes SPLs. Then SPLs, as transcription factors, up-regulated the miR397 and miR397 and further cause the down-regulation of its target genes. The red and blue arrows indicate up-regulation and down-regulation, respectively, as observed in the mRNA and small RNA sequencing in this study. SPL, SQUAMOSA promoter-binding protein-like. LAC, laccase.